GLIA 58:43–54 (2010)

Maintaining Retinal Astrocytes Normalizes Revascularization and Prevents Vascular Pathology Associated with Oxygen-Induced Retinopathy

MICHAEL I. DORRELL,[1] EDITH AGUILAR,[1] RUTH JACOBSON,[1] SUNIA A. TRAUGER,[2] JEFFREY FRIEDLANDER,[1] GARY SIUZDAK,[2] AND MARTIN FRIEDLANDER[1]*

[1]*Department of Cell Biology, The Scripps Research Institute, La Jolla, California*

[2]*Department of Molecular Biology, Scripps Center for Mass Spectrometry, The Scripps Research Institute, La Jolla, California*

KEY WORDS

retinal astrocytes; retinal neovascularization; progenitor cells

ABSTRACT

Astrocytes are well known modulators of normal developmental retinal vascularization. However, relatively little is known about the role of glial cells during pathological retinal neovascularization (NV), a leading contributor to vision loss in industrialized nations. We demonstrate that the loss of astrocytes and microglia directly correlates with the development of pathological NV in a mouse model of oxygen-induced retinopathy (OIR). These two distinct glial cell populations were found to have cooperative survival effects *in vitro* and *in vivo*. The intravitreal injection of myeloid progenitor cells, astrocytes, or astrocyte-conditioned media rescued endogenous astrocytes from degeneration that normally occurs within the hypoxic, vaso-obliterated retina following return to normoxia. Protection of the retinal astrocytes and microglia was directly correlated with accelerated revascularization of the normal retinal plexuses and reduction of pathological intravitreal NV normally associated with OIR. Using astrocyte-conditioned media, several factors were identified that may contribute to the observed astrocytic protection and subsequent normalization of the retinal vasculature, including vascular endothelial growth factor (VEGF) and basic fibroblast growth factor (bFGF). Injection of VEGF or bFGF at specific doses rescued the retinas from developing OIR-associated pathology, an effect that was also preceded by protection of endogenous glia from hypoxia-induced degeneration. Together, these data suggest that vascular-associated glia are also required for normalized revascularization of the hypoxic retina. Methods developed to target and protect glial cells may provide a novel strategy by which normalized revascularization can be promoted and the consequences of abnormal NV in retinal vascular diseases can be prevented.

INTRODUCTION

The abnormal growth of blood vessels and associated vascular leakage in diabetic retinopathy, exudative age-related macular degeneration, retinopathy of prematurity, and vascular occlusions are major causes of vision loss (Adamis et al., 1999; Das and McGuire, 2003; Friedlander, 2007). Numerous studies have demonstrated a role for vascular endothelial growth factor (VEGF) in the development of pathological neovascularization (NV) in the eye (Aiello et al., 1995; Caldwell et al., 2003; Ferrara and Kerbel, 2005; Ng et al., 2006; Witmer et al., 2003), and anti-VEGF drugs are currently in clinical use to slow down the progression of retinal vascular disease (Avery et al., 2006; Ng et al., 2006). However, potential problems with anti-VEGF therapy could limit its utility, including the need for repeated injections as well as potential secondary effects on other, non-endothelial cell types (Zachary, 2005). In addition to its role in angiogenesis and vascular permeability, VEGF has also been shown to have important neuroprotective activities in the retina (Robinson et al., 2001), and is a critical modulator of vascular associated cells such as astrocytes and microglia.

Cell-based therapy represents an emerging method by which vascular and neuronal degenerative diseases may be treated (Friedlander, 2005; Friedlander et al., 2007; Otani and Friedlander, 2005). Intravitreal injection of vascular-related progenitor cells prevents vascular regression and protects neurons in mouse models of retinal degeneration (Otani et al., 2002, 2004). Injection of myeloid progenitors facilitates vascular repair in models of ischemic retinopathy by accelerating normal revascularization of the superficial and deep retinal vascular plexuses, and decreasing intravitreal vascular pathogenesis (Ritter et al., 2006). These cell-based therapies have the potential to correct the underlying vascular abnormalities associated with ischemic retinopathies rather than simply treat the complications resulting from abnormal NV. While we have gained some insight regarding the vasculo- and neurotrophic properties of these cells, the precise mechanism by which they facilitate vascular rescue in models of ischemic retinopathy remains unclear.

The neovascular response to hypoxic stress in vascular disease models varies significantly from one mouse

Grant sponsor: National Eye Institute of the National Institutes of Health; Grant numbers: R01EY11254, R24EY017540; Grant sponsors: MacTel Foundation; V. Kann Rassmussen Foundation.

*Correspondence to: Martin Friedlander, Department of Cell Biology, The Scripps Research Institute MB-26, 10550 N. Torrey Pines Road, La Jolla, California 92037, USA. E-mail: friedlan@scripps.edu

Received 22 January 2009; Accepted 30 April 2009

DOI 10.1002/glia.20900

Published online 18 June 2009 in Wiley InterScience (www.interscience.wiley.com).

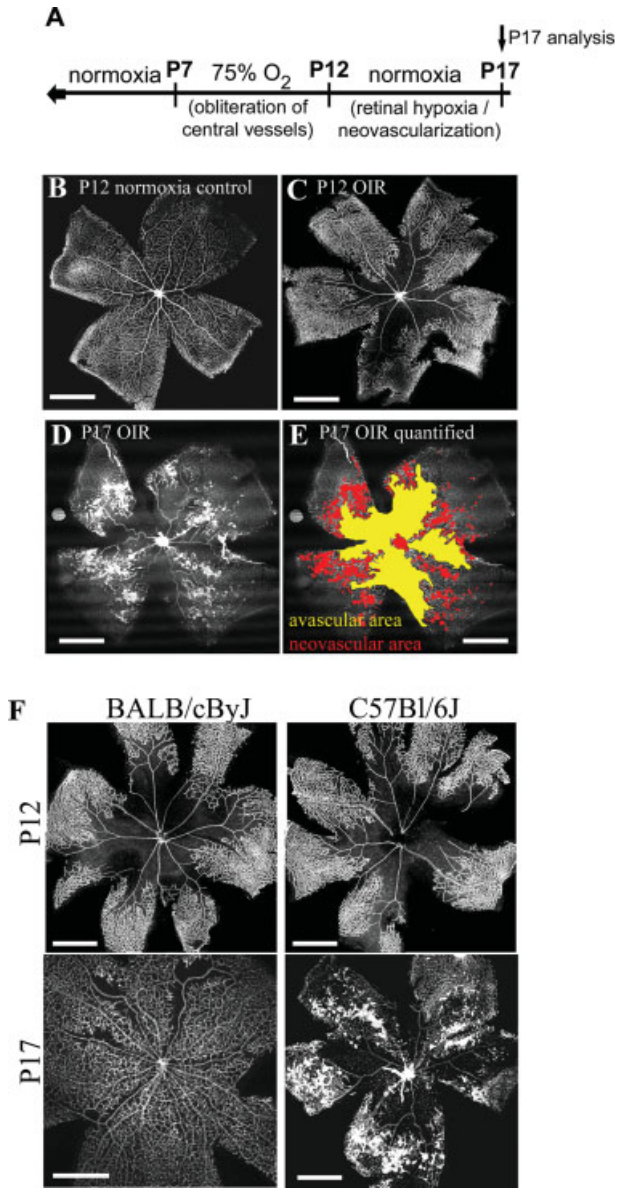

Fig. 1. BALB/cByJ and C57Bl/6J mouse strains react differently to OIR. (**A**) Mouse model of OIR: 7-day-old pups (post-natal day 7; P7) and their mothers are placed in 75% oxygen chambers for 5 days followed by return to ambient room air at P12. The retinas are analyzed at P17 when maximum pathology is observed in C57BL/6J mice. (**B**) Normal P12 retinas have a characteristic retinal vasculature that extends from the central retinal artery to the periphery and includes both superficial and deep vascular plexuses. (**C**) Exposure to hyperoxia from P7 to P12 results in attenuation of normal retinal vascular growth and obliteration of the central retinal vessels in mice. (**D**) Upon return to normoxia, the under-vascularized central retina becomes hypoxic leading to abnormal, pathological NV in C57BL/6J mouse retinas by P17. (**E**) The extent of normal revascularization can be quantified by measuring the remaining area of vascular obliteration at P17 (yellow) and the extent of pathological pre-laminar neovascularization (red). (**F**) BALB/cByJ and C57BL/6J mouse strains have different responses to the OIR model. Following 5 days of hyperoxia (P12), the extent of vaso-obliteration in the central retina is similar (top). However, by P17, normalized revascularization is completed in BALB/cByJ mouse retinas, while large areas of vaso-obliteration remain and increased pathology is observed in retinas from C57BL/6J mice (bottom). Size bars = 500 μm.

strain to the next (Rohan et al., 2000). This is exemplified by the response of albino BALB/cByJ and pigmented C57BL/6J mice to models of oxygen-induced retinopathy (OIR) (Ritter et al., 2006; Smith et al., 1994) (see Fig. 1). In the mouse OIR model, a transient period of hyperoxia during retinal vascular development causes the attenuation of normal retinal vessel development and degeneration of the newly formed, immature vasculature. Upon return to normoxia, the central retinal area where the vasculature has regressed becomes hypoxic leading to development of pathological NV at the interface between the perfused and non-perfused retina (Fig. 1A–E) (Smith et al., 1994). This model closely resembles retinopathy of prematurity (ROP), a condition which can be observed in premature infants who are placed in hyperoxic chambers thereby introducing the risk for developing retinopathy return to normoxia (Smith, 2002). In the OIR model, the retinal vasculature of both BALB/cByJ and C57BL/6J mice becomes obliterated to a similar extent during exposure to hyperoxia (Fig. 1F). However, in retinas from BALB/cByJ mice, the vascular obliterated regions revascularize more quickly, and pathological, pre-laminar neovascular tufts do not form. In contrast, the retinas of pigmented C57BL/6J mice are characterized by slower revascularization of the normal plexuses and the formation of pathological, pre-laminar neovascular tufts (Fig. 1F).

Astrocytes play a critical role during normal inner retinal vascularization (Dorrell et al., 2002; Fruttiger et al., 1996; Provis et al., 2000; Stone et al., 1995) and degeneration of retinal astrocytes in ischemic tissues is associated with failure of the blood retinal barrier in oxygen-induced retinopathies (Chan-Ling and Stone, 1992). In this study, we examine the potential role of astrocytes in OIR and explore the potential utility of cell therapy for the treatment of retinal ischemia. We demonstrate a strong correlation between astrocyte survival, rapid retinal revascularization, and lack of pathological NV in BALB/cByJ retinas when compared with retinas from C57BL/6J mice. We also describe trophic cross-talk between astrocytes and retinal microglia and provide evidence that the rescue potential of myeloid progenitor cells may, at least in part, be facilitated by protecting retinal astrocytes from degeneration in the C57BL/6J mouse retina. We further support a role of astrocytes in promoting normalized revascularization of the OIR retina by data demonstrating that other intervention strategies that protect the endogenous astrocytes from hypoxia-related degeneration, including the injection of astrocytes, astrocyte-conditioned media, and even low levels of VEGF or basic fibroblast growth factor (bFGF), also rescue the OIR phenotype. We therefore conclude that there is a strong correlation between astroglial survival and normalized retinal revascularization following oxygen-induced obliteration. This suggests a potential new therapeutic strategy for treating ischemic retinopathies that targets and rescues vasculature-associated glial cells rather than targeting and blocking the growth of vascular endothelial cells.

MATERIALS AND METHODS

Intravitreal Injections and the OIR Model

All animal protocols were approved by the IACUC committee at the Scripps Research Institute, La Jolla, CA. The OIR model was used as previously described (Banin et al., 2006; Smith et al., 1994). Briefly, post-natal day 7 (P7) pups and their mothers were exposed to 75% oxygen for 5 days and returned to normoxia at P12 (Fig. 1A). Exposure of the mouse pups to hyperoxia results in obliteration of the newly developed central retinal vessels (Fig. 1B,C). When the mice are returned to normoxia, the retina becomes hypoxic due to the absence of normal retinal vasculature, resulting in pathological neovascular growth by P17 (Fig. 1D,E). Appropriate cells (250,000 cells/eye), astrocyte-conditioned media, or various doses of bFGF or VEGF were injected intravitreally on post-natal day 7 (P7) or on post-natal day 12, as noted in Results and figure legends. Mice were euthanized and retinas isolated at various timepoints following return to normoxia. Following fixation using either 10 min of methanol at 4°C (GFAP) or 1 h of 4% paraformaldehyde (CD11b, isolectin GS), retinas were blocked for 2 h and stained for astrocytes using GFAP-specific antibodies (Sigma, St. Louis, MO; methanol fixation, 10 min), microglia using CD11b-specific antibodies (BD Biosciences, San Jose, CA), and/or vessels using the fluorescently conjugated isolectin *Griffonia Simplicifolia IB-4* (isolectin *GS*; Invitrogen). Isolectin GS can be used to effectively label murine endothelial cells and activated macrophages (Maddox et al., 1982), thus allowing us to differentiate resting microglia (CDllb positive) from activated macrophages (CDllb and lectin positive). Quantification of the remaining obliterated areas, used as a measure of the rate of normal retinal revascularization, and quantification of the areas of pathological neovascular growth were performed at P17 as previously described (Banin et al., 2006).

Isolation of Primary Astrocytes

Astrocytes were isolated using a published protocol (Gebicke-Haerter et al., 1989). Briefly, cerebral hemispheres were dissected from brains of neonatal mice. The dorsal cortex was isolated, avoiding the underlying white matter, and the tissue was minced in Hank's Balanced Salt Solution using forceps and by repeat pipeting with a P1000 pipette. After centrifugation at 1,000*g* for 5 min, 2.5 mL trypsin-EDTA (Invitrogen, Carlsbad, CA) per dissected brain was added and the tissue was dissociated at 37°C for 30 min followed by deactivation of the trypsin with an equal volume of growth media (DMEM +10% FBS + Glutamax + Pen-Strep; Invitrogen). The resulting cells were plated at low density in 75 cm^2 flasks and grown to confluency. These cells consisted mainly of astrocytes and microglia. To separate these two populations, the flasks were shaken in a culture chamber (humidified with 5% O_2) overnight at 225 rpm The microglia-containing media was removed leaving behind the attached astrocytes (approximately 95% pure), which were grown further and used within 3 passages. Alternatively, the astrocytic cell line, C8-D1A (ATCC) was used. These cells were grown in normal DMEM culture media containing 10% FBS. Primary or C8-D1A astrocytes were intravitreally injected at a concentration of 250,000 cells per eye using a 33-gauge needle and injecting a total volume of 0.5 μL per eye.

Isolation of Bone Marrow-Derived Myeloid Progenitor Cells

Whole bone marrow was isolated from the femurs and tibias of 6–8-week-old C57BL/6J mice. The isolated bone marrow cells were incubated with a fluorescently labeled antibody directed against CD44 (BD Biosciences–Pharmingen, clone IM7). Fluorescence-activated cell sorting (FACS) was performed on a FACSAria (BD) and was used to isolate $CD44^{hi}$ subpopulations that correspond to the myeloid progenitor fraction of the whole bone marrow (Ritter et al., 2006). Two hundred and fifty thousand cells per eye were injected intravitreally using a 33 gauge needle in a total volume of 0.5 μL per injection.

Injection of Astrocyte-Conditioned Media

Primary murine astrocytes or astrocytes from the murine C8-D1A cell line (ATCC) were grown in normal DMEM culture media containing 10% FBS until approximately 80% confluent. The cells were then washed thoroughly with PBS to remove any remaining serum followed by culture in serum-free DMEM. After 7 days, the astrocyte-conditioned, serum-free media was collected and cellular debris was removed by centrifugation at 5,000*g* for 5 min. The remaining supernatant was collected and concentrated 100-fold using 10 kDa molecular weight cutoff centrifuge filters (Pierce). The 100× concentrated astrocyte-conditioned media was injected intravitreally in 0.5 μL volumes. Control, non-conditioned serum-free DMEM media was also concentrated 100-fold and injected intravitreally in 0.5 μL volumes as a negative control.

Semi-Quantification of Astrocyte Rescue in the Retinal Vascular Obliterated Areas

The extent of astrocyte persistence in the vascular obliterated areas was quantified by analyzing the OIR retinas at P14, 2 days following removal from hyperoxia. Retinas were dissected, flat-mounted, and stained for GFAP to visualize the astrocytes. Masked observers scored the extent of astrocyte persistence in the obliterated zones on a 0–6 scale. Values of 0 or 1 indicated that no or very few astrocytes were observed in the vascular obliterated zone. Values of 2–4 indicated retinas with substantial numbers of astrocytes remaining in the vascular obliterated zones (although still fewer than nor-

mal), but indicated that these astrocytes appeared abnormal, lacked the normal cellular processes, and the standard network observed in a normal astrocytic template was not observed. Values of 5 and 6 indicated retinas with large numbers of astrocytes which were observed to form a mostly to completely normal astrocytic template within the vascular obliterated zones.

Western Blot and Proteomic Analysis

Serum-free astrocyte-conditioned media was collected and concentrated 100-fold as described for the intravitreal injections. Twenty-microliter samples of the concentrated conditioned media or concentrated non-conditioned control media were then separated by polyacrylamide gel electrophoresis. After Coomassie staining, prominent bands were cut using sterile technique and analyzed by LC-MS/MS mass spectrometry to identify proteins in the astrocyte-conditioned media. In separate gels, the samples were transferred to nitrocellulose paper. After blocking with 5% milk buffer in PBS + 0.1% Tween, the blots were incubated with rabbit anti-mouse bFGF (NOVUS, 008-100) or rabbit anti-mouse pan VEGF (Chemicon, AB1876). The blots were then washed, incubated with HRP conjugated secondary antibodies, washed again, and visualized by chemiluminescence (Pierce, 34075).

LC-MS/MS Analysis

Proteins were solubilized in 0.1% Rapigest (Waters Corportation) and reduced in 10 mM D,L-dithiothrietol (Sigma) for 1 h followed by alkylation with 55 mM iodoacetamide (Sigma) for 30 min in the dark. Proteins were trypsin digested at 37°C using a 1:30 (w/w) enzyme to substrate ratio. The peptides were analyzed by reverse phase chromatography prior to mass spectrometry analysis using Zorbax SB-C18 stationary phase (Agilent; 5 μm particles, 15 cm length, 75 μm inner diameter). The reverse phase gradient separation was performed using water and acetonitrile (0.1% formic acid) mobile phase gradients.

The data-dependent MS/MS data was obtained on a LTQ linear ion trap mass spectrometer using a home built nanoelectrospray source. One MS spectrum was followed by 4 MS/MS scans on the most abundant ions after the application of the dynamic exclusion list. Protein identification was performed using Mascot (Matrix Science, London, UK; version 2.1.04) at the 95% confidence level with a calculated false positive rate of <1% as determined using a reversed concatenated protein database.

Tandem mass spectra were extracted by the Xcalibur software. All MS/MS samples were analyzed using Mascot (Matrix Science, London, UK; version 2.1.04). Scaffold (version Scaffold-01_06_03, Proteome Software, Inc., Portland, OR) was used to additionally validate MS/MS based peptide and protein identifications. Peptide identifications were accepted if they could be established at greater than 95.0% probability as specified by the Peptide Prophet algorithm (Keller et al., 2002). Protein identifications were accepted if they could be established at greater than 99.0% probability and contained at least 2 identified peptides.

RESULTS

Astrocyte and Microglia Loss in the Hypoxic Retina Correlates with OIR Pathology

Over the past two decades, models of OIR have become common for studying hypoxia-induced angiogenesis (Chan-Ling and Stone, 1992; Madan and Penn, 2003; McLeod et al., 1998; Penn et al., 1993; Smith et al., 1994). Vascular changes observed in the mouse model of OIR are consistent, reproducible, and quantifiable (Banin et al., 2006), and its use has been extended to the study of angiogenesis in general, as well as testing various angiostatic molecules (Eichler et al., 2006; Ferrara and Kerbel, 2005). We analyzed two strains of mice, BALB/cByJ and C57BL/6J, for differences in the response of vascular-related cells in OIR. As previously noted (Ritter et al., 2006), retinas from both strains demonstrated equal levels of hyperoxia-induced vascular obliteration. However, the retinal vascular response to the ensuing hypoxia after removal from hyperoxia was dramatically different in the two strains (Fig. 1F). The retinal vasculature of BALB/cByJ mice revascularized rapidly reproducing the characteristic superficial and deep vascular plexuses without pathological NV by 5 days post-hyperoxia (P17). In contrast, retinas of C57BL/6J mice exhibited slower revascularization of the normal retinal plexuses and extensive pathological NV (Fig. 1F).

We next analyzed the retinal astrocytes to determine if there were also strain differences in the survival and persistence of retinal astroglia. In both BALB/cByJ and C57BL/6J mice, retinal astrocytes survived through hyperoxia and were observed in the vaso-obliterated areas upon return to normoxia at P12 (Fig. 2A). In retinas from C57BL/6J mice, astrocytes in the vaso-obliterated zone quickly began to degenerate and were mostly absent by 48 h following return to normoxia (P14) (Fig. 2B,C). The loss of astrocytes is accompanied by an increase in Müller cell GFAP reactivity which is observed as spotted staining from the Müller cell endfeet within the superficial vascular plexus. These activated Müller glia are observed as GFAP positive cells with processes spanning the entire retina (Fig. 2D). Activation of Müller glia and subsequent GFAP reactivity is commonly associated with retinal stress and vascular disease (Dorrell et al., 2009; Rungger-Brandle et al., 2000). In contrast, astrocytic density remained high within the vaso-obliterated zone of retinas from BALB/cByJ throughout revascularization and Müller cell activation was not observed (Fig. 2B,C). Thus, astroglia survival correlates with accelerated physiological revascularization and decreased pathological changes in

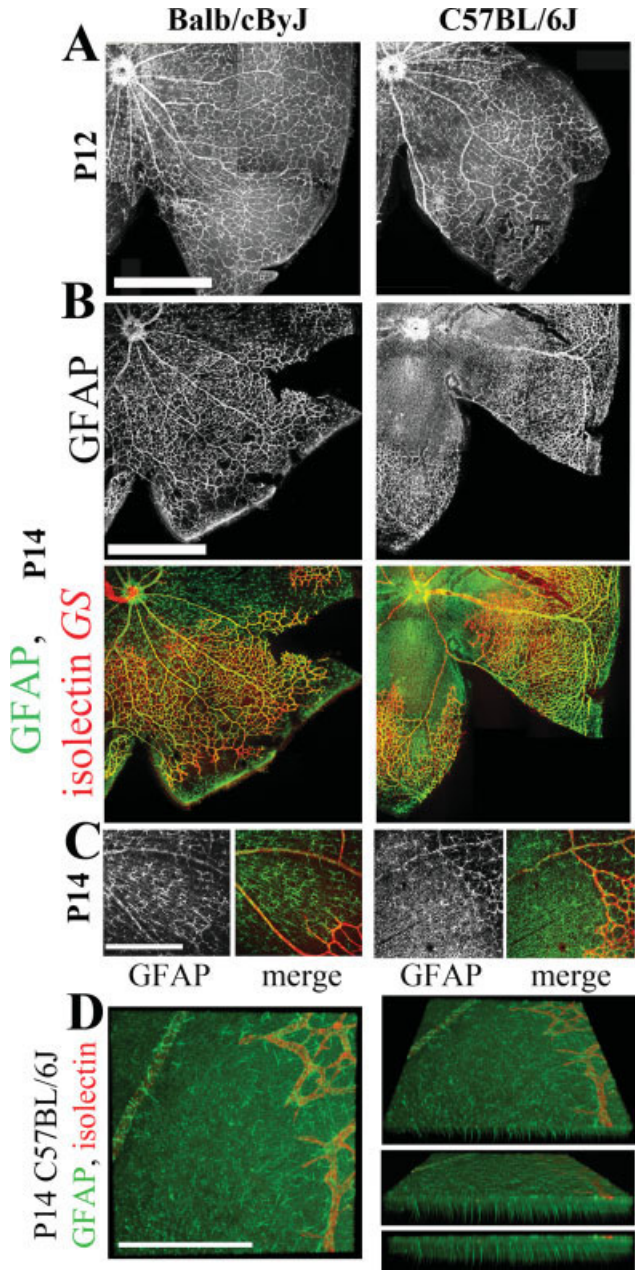

Fig. 2. Astrocyte degeneration correlates with subsequent pathology in the avascular, hypoxic areas of the central OIR retina following return to normoxia. (**A**) Staining with GFAP demonstrates the presence of astrocytes in the vaso-obliterated areas of retinas from both C57Bl/6J and BALB/cByJ strains of mice at P12, immediately after return from hyperoxia to normoxia. (**B**) Astroctyes are maintained within the vaso-obliterated areas of BALB/cByJ mice at P14, but have degenerated by P14 in the vaso-obliterated zone of C57BL/6J mice. The punctate GFAP staining within the obliterated zone of C57BL/6J mice represents the inner endfeet of activated Müller glia. (**C**) Higher magnification images of the interface between the vascularized and vaso-obliterated zones showing strain differences in astrocyte persistence and Müller glia activation at P14 of the OIR model. (**D**) 3-dimentional renderings demonstrate GFAP staining of the characteristic trans-retinal processes of activated Müller glia and show association with the punctate staining observed within the superficial plexus of C57BL/6J retinae. All four images are of the same region, but rotated around the *Y* axis by 0° (left), 30° (top right), 60° (middle right), and 90° (bottom right). Size bars = 500 μm (A, B), 100 μm (C, D).

the BALB/cByJ mouse retinas. Differences in myeloid cell persistence have also been observed in the BALB/cByJ and C57BL/6J mouse retinas following OIR (Ritter et al., 2006). These results suggest that the persistence of retinal astrocytes and microglia within the vaso-obliterated areas may help facilitate normal revascularization, as observed in the BALB/cByJ strain, whereas their degeneration may contribute to the pathological neovascularization normally observed in the C57BL/6J mouse retina.

Injection of BM-MPCs Mediates Astrocyte Survival in C57BL/6J Mice

We have previously demonstrated that intravitreal injection of bone marrow-derived myeloid progenitor cells (BM-MPCs) leads to enhanced physiological revascularization and reduced pathological NV in C57BL/6J mouse retinas following hyperoxia, resulting in a phenotype that more closely resembles that of BALB/cByJ mice (Ritter et al., 2006) (Fig. 3A). Based on our findings that correlate astrocyte persistence in the retina with accelerated physiological revascularization and reduced pathology, we tested whether BM-MPCs also protected astrocytes from degeneration within the hypoxic, vascular-obliterated zones of C57BL/6J retinas following OIR. Injection of BM-MPCs at P7 resulted in astrocyte survival and maintenance of a relatively normal astrocytic template within the vaso-obliterated central retina (Fig. 3B,C). This was correlated with accelerated revascularization of the normal retinal plexuses and reduced pathological NV. These results also support a correlation between astrocyte survival and normal revascularization of the ischemic retina; astrocyte survival at P14 occurred in retinas with BM-MPC treatment which subsequently resulted in a normalized vascular phenotype by P17. Vehicle (PBS) control injection also rescued the astrocytes from degeneration compared with non-injected OIR controls (Fig. 3C), but at significantly lower levels than observed with BM-MPC injection. This correlates with a slight OIR rescue consistently observed by vehicle or sham injection compared with non-injected retinas (Ritter et al., 2006).

Astrocytes Mediate Survival of Myeloid Cells and Endogenous Astrocytes

Bone-marrow derived progenitor cells target specifically to sites of gliosis, reactive astrocyte activity and growth (Dorrell et al., 2004; Otani et al., 2002). Having demonstrated that BM-MPC injections promote astrocyte and vascular rescue, presumably by replacing the degenerated microglia population and protecting the endogenous astrocytes from degeneration, we next tested whether intravitreal injection of astrocytes can also promote cell survival and facilitate physiological revascularization in the OIR model. Both primary astrocytes, isolated from neonatal mouse brains, and the

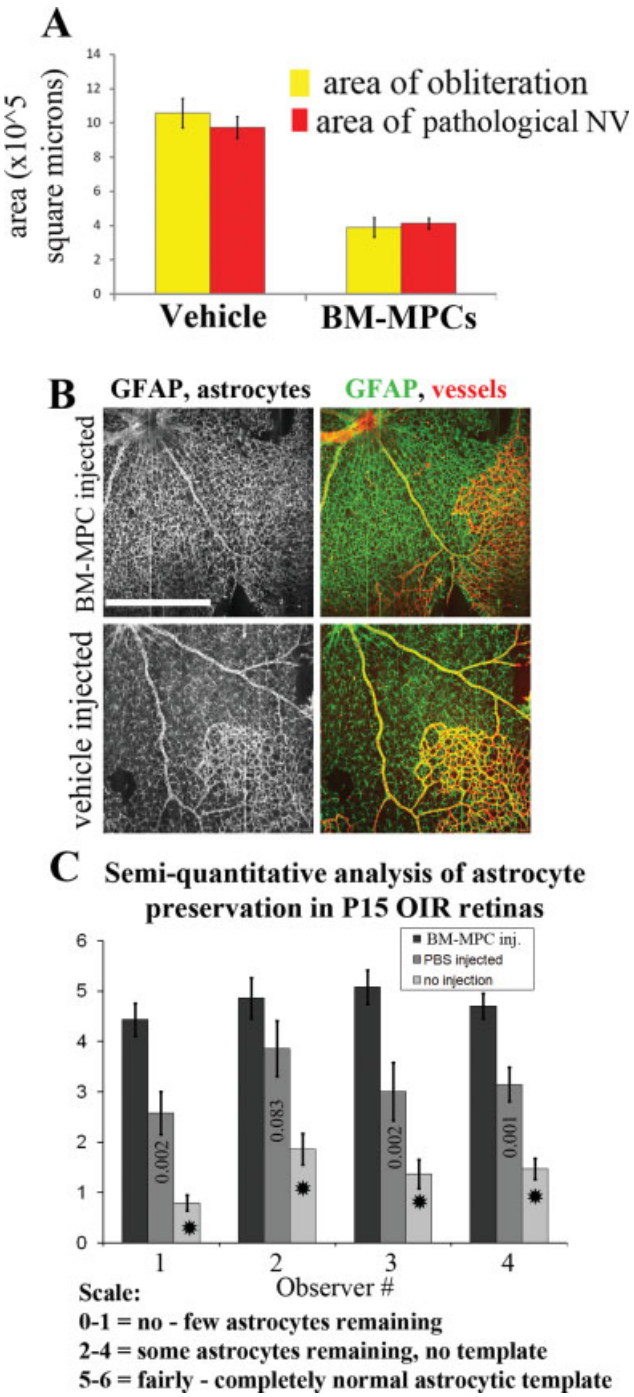

Fig. 3. Injected bone marrow-derived myeloid progenitor cells (BM-MPCs) protect retinal astrocytes and rescue the retinal vasculature following OIR. (**A**) Injected BM-MPCs rescue the OIR phenotype by reducing the area of obliteration in C57BL/6J retinas at P17 (demonstrating accelerated revascularization of the normal retinal plexuses), while reducing the formation of pathological neovascular tufts (cumulative data; *N*s > 60; *P* values < 0.001). (**B**) The vascular rescue is associated with protection of the endogenous astrocytes within the vascular obliterated zones at P14. (**C**) Injection of BM-MPCs significantly increases astrocyte persistence compared with vehicle or non-injected retinas (*N* = 12 for each condition; *P* values comparing each treatment to vehicle injected or non-injected levels are as indicated (stars indicate *P* values <0.0001)). Size bars = 100 μm.

astrocytic cell line C8-D1A promoted growth of myeloid cells *in vitro*. BM-MPCs survived and proliferated in co-culture with astrocytes whereas the same cells did not survive using comparable culture conditions without astrocytes (Fig. 4A). Serum-free media pre-conditioned by astrocytes also facilitated myeloid progenitor cell growth *in vitro*, suggesting that myeloid cell survival is facilitated by astrocyte secreted factors. Thus, it appears that the trophic effects of astrocytes and the BM-MCPs occurs in a reciprocal manner, at least *in vitro*.

Having demonstrated that the persistence of astrocytes and microglia within the vascular obliterated zones of the OIR retinas was highly correlated with normalized revascularization, we wanted to determine if astrocytes or astrocyte conditioned media could also protect microglia and endogenous astrocytes *in vivo*. Intravitreal injection of astrocytes into C57BL/6J OIR mice at P7 led to increased density of the endogenous microglia (CD11b) and the presence of activated macrophages within the vaso-obliterated zones at P14 (2 days following removal from OIR). As previously observed, microglia were present upon removal from hyperoxia but were substantially reduced by P14 within the hypoxic, vascular-obliterated zones of control injected C57BL/6J OIR mice (Fig. 4B). Relatively normal astrocytic templates were also observed following astroglia cell injections indicating that these treatments also promote survival of endogenous astrocytes. Similar to the results observed following injection of astrocytes, injection of astrocyte-conditioned media also promoted survival of the endogenous microglia and maintenance of the endogenous astrocytic template within the vascular-obliterated zones of C57BL/6J retinas (Fig. 4B,C). Based on semi-quantitative scores from each of four masked observer's, astrocyte survival within the vascular obliterated zones of OIR retinas was significantly enhanced in retinas injected with astrocyte-conditioned media (Fig. 4C). These data demonstrate that astrocyte-secreted factors promote the survival of myeloid cells *in vitro*, and endogenous retinal microglia and astroglia *in vivo*.

Intravitreal Injection of Astrocytes Mediates Rescue of the OIR Phenotype

We next determined whether intravitreal injection of astrocytes also resulted in modified retinal vasculature following OIR. Injection of either C8-D1A astrocytes or primary astrocytes at P7 (prior to exposure to hyperoxia) protected the retinas from the pathological changes observed in OIR to an extent comparable to that observed when BM-MPCs were injected (Fig. 4D,E). Revascularization of the normal retinal plexuses was accelerated, as demonstrated by a decrease in the remaining vaso-obliterated areas at P17, and pathological NV was also inhibited, as shown by a decrease in areas of neovascular tuft formation. It is important to note that the extent of vascular obliteration between all retinas was identical at P12, indicating that these cells did not pre-

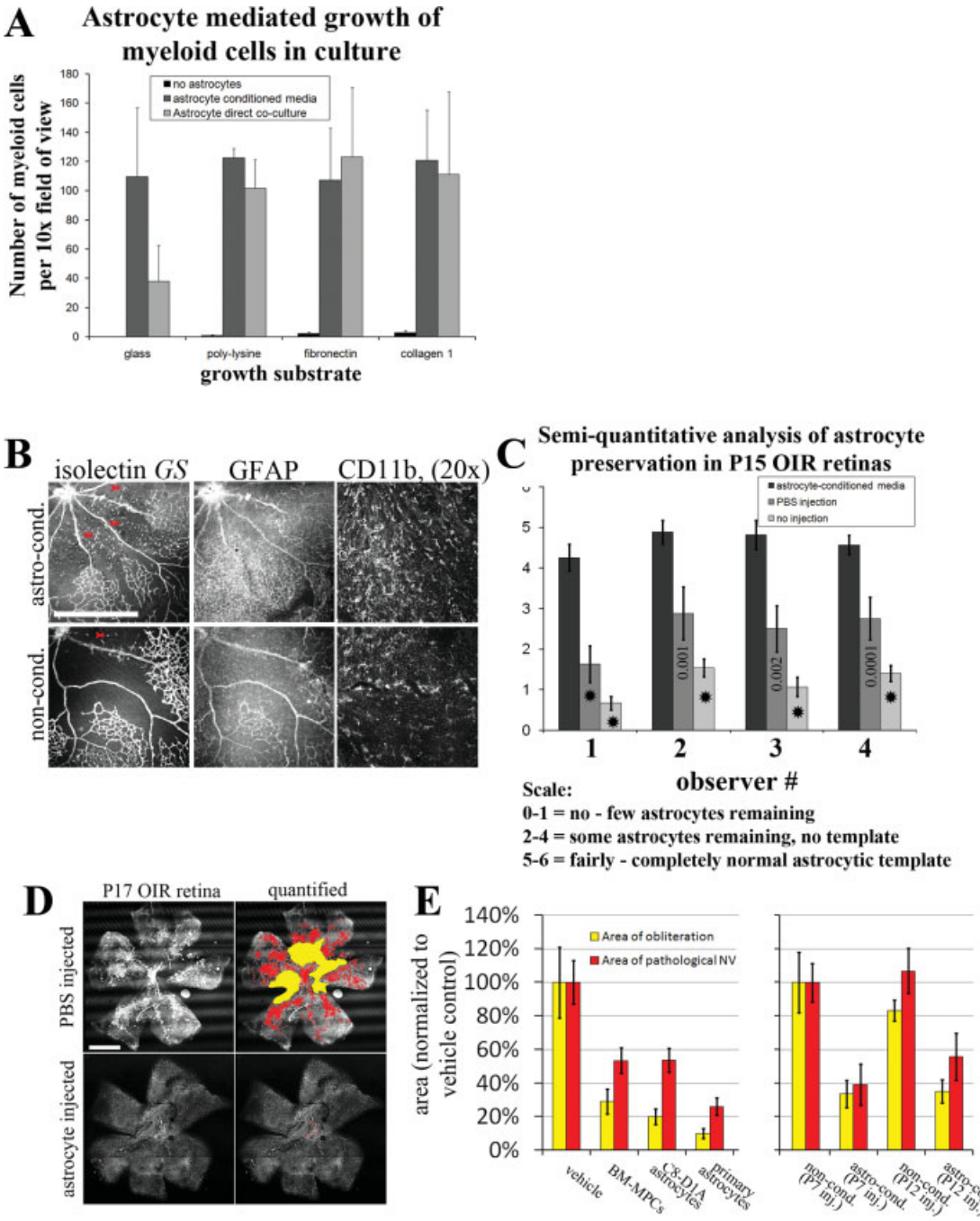

Fig. 4. Injection of astrocytes or astrocyte-conditioned media results in normalized revascularization in the OIR model. (**A**) Astrocytes facilitate growth and survival of BM-MPCs in culture. (**B**) Injection of astrocyte-conditioned media results in persistence of isolectin *GS*-labeled activated macrophages (left; red arrows), GFAP positive astrocytes (middle) and CD11b positive microglia (right) within the hypoxic, vascular obliterated regions of C57BL/6J retinas compared with injection of control, non-conditioned media. (**C**) Astrocyte-conditioned media significantly protects endogenous astrocytes in the OIR model ($N = 16$: astrocyte-conditioned media and no-injection controls; $N = 12$: vehicle injected controls; P values comparing each treatment to vehicle injected or non-injected levels are as indicated (stars indicate P values <0.0001)). (**D**, **E**) At P17, injection of astrocytes or astrocyte-conditioned media accelerates normalized revascularization and prevents pathological neovascular tuft formation at levels equivalent or better than the injected BM-MPCs ($N = 12$ for each condition; all P values <0.001 for each treatment compared with the appropriate vehicle control). Size bars = 100 μm.

vent hyperoxia-induced vaso-obliteration, but rather accelerated subsequent revascularization of the normal retinal vascular plexuses. Injection of astrocytes did not lead to any adverse immune reactions or formation of intraocular tumors. In contrast, other cell types such as primary fibroblasts demonstrated no evidence of vascular rescue and injection of non-differentiated mouse embryonic stem cells resulted in massive inflammation and retinal toxicity due to extensive, uncontrolled growth of these cells (data not shown).

TABLE 1. Molecules Identified in the Astrocyte-Conditioned, Serum-Free Media

Angiogenesis
ADAMTS 1
Angiopoietin-related protein 2
Basic fibroblast growth factor (bFGF)
Lactadherin
PEDF
Periostin
Phosphoglycerate kinase
Thrombospondin
TIMP-2
Vascular endothelial growth factor (VEGF)
Antioxidant
Superoxide dismutase
Cell adhesion
CD9
Integrin alpha-6
Meosin
N-Cadherin
Neural cell adhesion molecule
SPARC-like protein
Cytokine signaling related
14-3-3 protein
BMP-1
Calayntenin
Carboxypeptidase E
GDNF family receptor alpha-2
Glia maturation factor
Hepatocyte growth factor receptor
IGF BP-7
IGF-2
Latent TGF-binding protein 4
Meteorin
Neogenin
Nucleoside diphosphate kinase B
PDGF-A
Programmed cell death 6-interacting protein
Sulfated glycoprotein 1
TGF-beta 2
Tyrosine protein kinase receptor UFO
ECM
Collagen alpha-1
Dystroglycan
EGF-containing fibulin-like ECM protein 2
Epsilon-sarcoglycan precursor
Fibronectin
Glypican-1
Heparin sulfate proteoglycan
Laminin alpha-4
Laminin beta-1
Laminin beta-2
Laminin gamma-1
Lysyl oxidase homolog 3
MMP-19
TGF-beta glycoprotein ig-h3
Tubulointerstitial nephritis antigen
Xylosyltransferase 1
Inflammation and coagulation
Amyloid beta A4
Annexin A1
Annexin A5
Antithrombin 3
CD81
Complement C4
Renin receptor
Vitamin k dependent protein
Lipid transport
Apolipoprotein D
Epidermal FABP
LDL receptor
Phospholipid transfer protein
Protease related
6-Phosphogluconolactonase
Cathepsin B
Glia derived nexin precursor
Serine protease inhibitor A3N
Protein transport/folding
78-kDa glucose regulating protein
Calumenin
HSP 71kDa
HSP70
HSP-90
Transcobalamin II

Intravitreally injected BM-MPCs target the retina in large numbers (Ritter et al., 2006). In contrast, when we injected primary astrocytes obtained from eGFP mice, very few of the injected astrocytes became localized to the retina following intravitreal injection. The majority of injected astrocytes remained in the vitreous (data not shown). Despite this, astrocytes effectively normalized the vascular phenotype in the C57Bl/6J OIR retinas at levels similar to the retina-targeting BM-MPCs (Fig. 4E), indicating that retinal targeting and direct cell–cell contact is not required for astrocyte-mediated rescue. This suggests that the injected astrocytes may secrete factors that mediate the observed rescue effects. To test this further, we injected serum-free media preconditioned by C8-D1A astrocytes and analyzed the effects on the retinal vasculature of C57BL/6J mice after OIR. Injection of astrocyte-conditioned serum-free media also resulted in vascular rescue as demonstrated by accelerated revascularization of the normal retinal plexuses and reduced intravitreal pathological NV. This effect was observed whether the astrocyte-conditioned media was injected at P7 (just prior to exposure to hyperoxia) or at P12 (upon return to normoxia) (Fig. 4D). This result is consistent with our earlier findings demonstrating that astrocyte-conditioned media facilitated survival of both microglia and astrocytes in the vaso-obliterated zones of OIR retinas. These data further strengthen the correlation between astrocyte and microglial survival and normalized revascularization in the OIR model.

Injection of bFGF or VEGF Rescues the OIR Phenotype

To determine what secreted factor(s) might mediate the OIR rescue effect, we analyzed the serum-free, conditioned media using LC-MS/MS proteomics. Several molecules were identified in the astrocyte-conditioned, serum-free media (Table 1). Multiple extracellular matrix molecules were found, along with cell adhesion molecules and various molecules involved in protein transport and folding. Several secreted molecules were also identified, including vascular-related molecules such as bFGF, VEGF, several other cytokine and signaling-related molecules, and molecules involved in coagulation or inflammation (Table 1). The presence of bFGF and VEGF in the conditioned media was confirmed by western blot analysis (Fig. 5A).

Both astrocytes (Araujo and Cotman, 1992) and microglia (Liu et al., 1998) are known to express bFGF and astrocytic expression of bFGF can protect endothelial cells from oxygen-induced degeneration in the mouse OIR model (Yamada et al., 2000). However, we have shown rescue effects resulting from injection of astrocyte-conditioned media at P12, after the mice return from hyperoxia and after vascular obliteration is complete. To test the possibility that bFGF might participate in the astrocyte-mediated vascular rescue effect, varying levels of bFGF were intravitreally injected into OIR mice at P12. Low doses (10 or 30 ng per eye) of bFGF

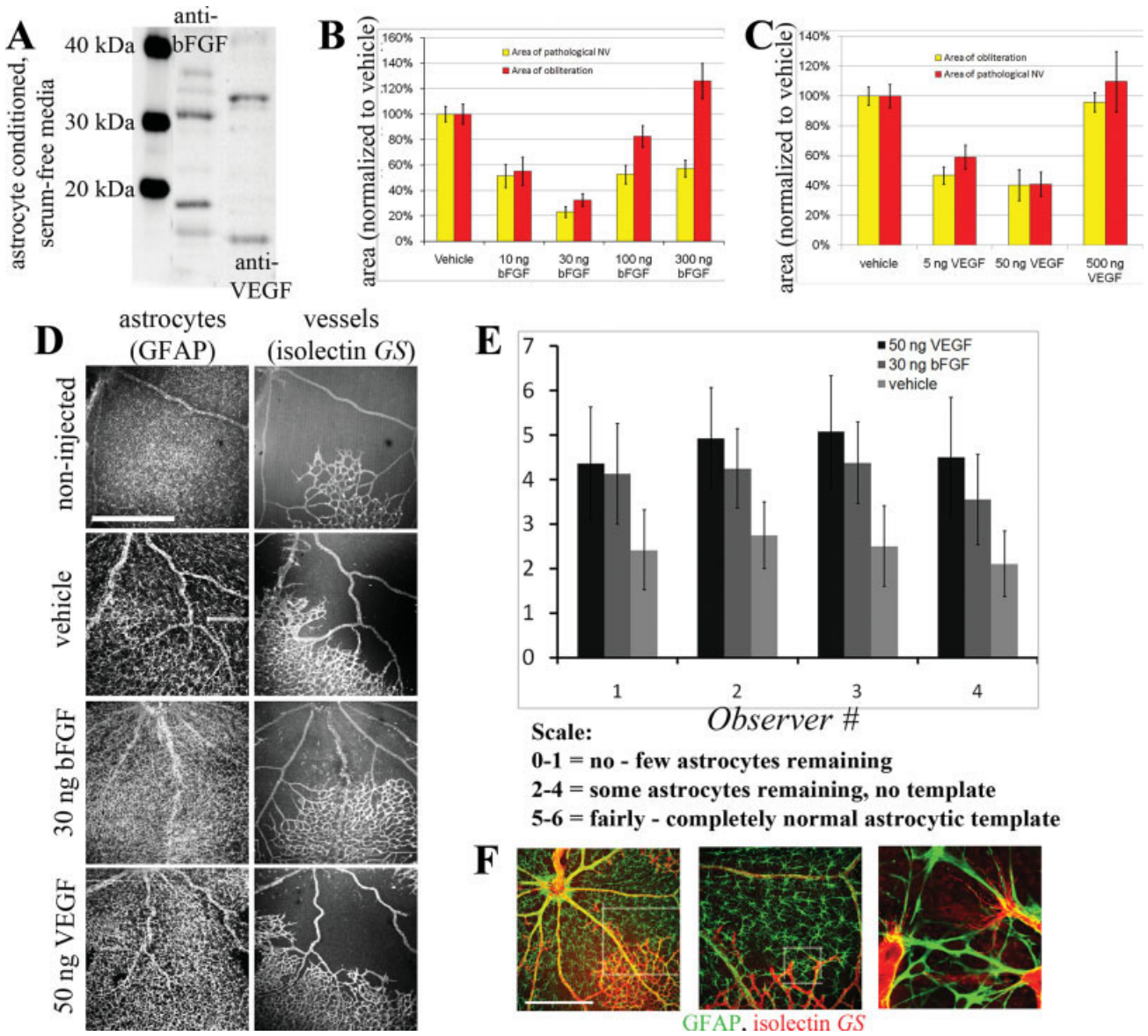

Fig. 5. Injection of small quantities of bFGF or VEGF can protect retinal astrocytes and rescue the retinal vasculature in the OIR model. (**A**) bFGF and VEGF is secreted by astrocytes and is present in the astrocyte-conditioned, serum-free media. (**B**, **C**) Injection of bFGF (B) or VEGF (C) can rescue the retinal vasculature in the OIR model in a dose dependent manner ($N \geq 10$ for each condition). (**D**) The observed vascular rescue effects are preceded by protection of the endogenous astrocytes from hypoxia-induced degeneration within the vascular obliterated zones at P14. (**E**) Quantification of the observed astrocytic rescue effects ($N \geq 10$ for each condition; for all observers P values ≤ 0.001 for bFGF or VEGF compared with vehicle injection). (**F**) Filopodia are extended from the endothelial cells planar to the protected astrocytes within the vaso-obliterated retina. These extensions can mediate potential guidance along the astrocytic template and suggest an explanation for the observed normalized revascularization associated with astrocyte protection in the vaso-obliterated zone. Each slightly opaque square indicates the area shown in the adjacent, higher magnification image. Size bars = 100 μm.

mediated accelerated revascularization of the obliterated areas in a dose dependent manner and inhibited neovascular tuft formation (Fig. 5B). Injection of 30 ng bFGF per eye was optimal while injection of lower or higher doses of bFGF was less effective (Fig. 5B).

VEGF was also injected at varying doses for comparison with bFGF injection. Astrocyte secretion of VEGF is known to mediate retinal vascular development (Gerhardt et al., 2003; Provis et al., 1997; Stone et al., 1995). However, overexpression of VEGF during the ischemic phase of OIR is also known to be a critical driving factor in the formation of pathology (McLeod et al., 2002; Smith et al., 1999; Werdich et al., 2004) and blocking VEGF activity has proven to be effective in preventing OIR-induced pathological neovascularization (Aiello et al., 1995; Ishida et al., 2003; Ng et al., 2006; Ozaki et al., 2000). Surprisingly, we found that injection of VEGF at relatively low levels actually rescued the OIR phenotype by enhancing revascularization and reducing areas of neovascular tufts (Fig. 5C). Similar to injection

of bFGF, injection of higher doses of VEGF no longer rescued the C57BL/6J OIR phenotype (Fig. 5C). Injection of the optimal concentrations of either bFGF (30 ng/eye) or VEGF (50 ng/eye), were found to significantly increase survival of the retinal astrocytes within the obliterated vascular zone (Fig. 5D,E), again demonstrating a correlation between astrocyte survival with accelerated revascularization and reduced OIR pathology.

DISCUSSION

Strong associations exist between retinal blood vessels and vascular associated cells such as astrocytes, microglia, and pericytes. Retinal astrocytes play a critical role during normal retinal vascular development by expressing VEGF and initiating endothelial cell proliferation (Provis et al., 1997; Stalmans et al., 2002; Stone et al., 1995). Endothelial cell guidance along the underlying astrocytic template during retinal vascular development is mediated by specific VEGF isoforms expressed by retinal astrocytes (Gerhardt et al., 2003; Stalmans et al., 2002) and specific R-cadherin mediated cell–cell adhesion (Dorrell and Friedlander, 2006; Dorrell et al., 2002). It is likely that astrocytes also play an important role in promoting normal revascularization during ischemic injury (Chan-Ling and Stone, 1992).

We have demonstrated that normalized revascularization of the vaso-obliterated retina in the mouse OIR model strongly correlates with the survival of astroglia and microglia during hypoxic insult. In each case, astrocyte and microglia survival within the vaso-obliterated, hypoxic retina correlates with accelerated revascularization of the normal retinal plexuses and reduced pathological intravitreal NV. Vascular degeneration in the central retinal vasculature is similar in both BALB/cByJ and C57Bl/6J mouse retinas after exposure to hyperoxia. Therefore, the neovascular drive is likely to be comparable in the two strains upon return to normoxia. However, in BALB/cByJ mice, the retinal astrocytes and retinal microglia survive within the vaso- obliterated areas of the retina following return to normoxia. Subsequently, normal retinal revascularization occurs much more quickly and without formation of pathological pre-retinal NV. In C57Bl/6J mice, the retinal astrocytes and retinal microglia disappear from the avascular, hypoxic areas of the retina and this is associated with slower recovery and formation of large pathological, pre-retinal vascular tufts.

The correlation between the survival of astrocytes within the hypoxic, vaso-obliterated areas after return to normoxia and subsequent revascularization in the mouse OIR model is also demonstrated by analyzing treatments that preserve the endogenous astrocytic template and subsequently normalize retinal revascularization. We hypothesize that in the absence of astrocytes, no template remains to guide blood vessel growth during the revascularization resulting in disorganized vessels and the formation of pathological, intravitreal NV. However, when astrocytes survive within the central vaso-obliterated retina, the remaining astrocytic template facilitates normalized revascularization of the characteristic retinal vascular plexuses. Endothelial filopodia can be observed extended along the astrocytic template (Fig. 5F) during revascularization suggesting that the vessels are indeed identifying underlying guidance cues provided by the astrocytes. This facilitates similar retinal vascular guidance mechanisms to those that initially produce the characteristic vascular plexuses during development, a process known to be mediated by endothelial filopodia and astrocytic guidance cues (Dorrell et al., 2002; Fruttiger et al., 1996; Gerhardt et al., 2003). BM-MPCs, astrocytes and astrocyte-conditioned media all protect the endogenous astrocytes and subsequently promote normalized revascularization in C57BL/6J mouse retinas.

Proteomic analysis of the astrocyte-conditioned media was used to identify proteins that may mediate the rescue effect (Table 1). Both bFGF and VEGF were identified in the astrocyte-conditioned media (see Fig. 4) and are known to be secreted by retinal astrocytes and microglia (Scherer and Schnitzer, 1994; Yamada et al., 2000). We have demonstrated that intravitreal injection of either bFGF or VEGF at low doses mimics the astrocyte and astrocyte-conditioned media-mediated rescue effects. It is unlikely that such therapy would be used to treat vascular-associated retinopathies since both bFGF and VEGF are known to contribute to neovascularization in these diseases. In fact, most therapies currently used to treat ischemic retinopathies are designed to inhibit their activity. However, our data demonstrates that at specific doses, these growth factors can actually have beneficial effects, presumably by protecting critical vascular-related glial cells from hypoxia-induced cell death. Our data suggests that it is important to consider possible detrimental effects that treatments blocking similar growth factors might have on vascular-related cells such as microglia and astrocytes. Inhibition of VEGF or bFGF certainly can block endothelial cell proliferation and reduce vascular permeability (Aiello et al., 1995; Caldwell et al., 2003; Witmer et al., 2003), but may also lead to loss of the important microglia and astrocytes as well, resulting in potential long-term repercussions. Thus, it may be important to identify other potential therapies to treat ischemic diseases of the eye.

Cell-based therapy may be one avenue by which ocular vascular diseases can be treated in the future. Recently, a population of Müller glia were found that can function as neuronal stem cells (Bernardos et al., 2007). Perhaps, in the future, these cells or other glial progenitors may be found that can replace lost astrocytes. In the meantime, cell therapy with astrocytes or myeloid progenitors may be a useful approach since these cells can react to the local environment, potentially secrete appropriate levels of growth factors important for normalized vascular regrowth, and lead to retinal vascular stabilization. Astrocyte injection rescues the vascular phenotype whereas other cell types such as fibroblasts or embryonic stem cells have no effect. However, we do not observe incorporation of the

injected astrocytes into the retina. Thus, the use of astrocytes as a long-term cell therapy in cases of continuing ischemia may not be practical. Previous studies from our laboratory have demonstrated that intravitreal injection of bone marrow-derived myeloid progenitor cells (BM-MPCs) leads to accelerated and normalized revascularization, as well as inhibition of pathological NV following hyperoxia-induced vascular obliteration in the mouse OIR model (Ritter et al., 2006). We now demonstrate that this vascular rescue is preceded by BM-MPC mediated rescue of retinal astrocytes within the vascular obliterated zones of C57Bl/6J mouse retinas, suggesting a potential mechanism of action for the observed rescue activity. By preventing astrocyte cell death in the hypoxic zones, and re-populating the central retina with microglia, the BM-MPCs may help facilitate normalized revascularization of the central retina in C57/Bl-6 mice which would otherwise develop pathological NV. Myeloid progenitors incorporate into the retina and become functionally active microglia and thus may have continued, long-term beneficial effects on the survival of critical vascular-associated glial cells. This may provide a paradigm for long-term therapy which can normalize revascularization of the ischemic retina and alleviate problems associated with the underlying disease.

ACKNOWLEDGMENTS

M.I.D. was supported by a fellowship from the California Institute for Regenerative Medicine (CIRM).

REFERENCES

Adamis AP, Aiello LP, D'Amato RA. 1999. Angiogenesis and ophthalmic disease. Angiogenesis 3:9–14.

Aiello LP, Pierce EA, Foley ED, Takagi H, Chen H, Riddle L, Ferrara N, King GL, Smith LE. 1995. Suppression of retinal neovascularization in vivo by inhibition of vascular endothelial growth factor (VEGF) using soluble VEGF-receptor chimeric proteins. Proc Natl Acad Sci USA 92:10457–10461.

Araujo DM, Cotman CW. 1992. Basic FGF in astroglial, microglial, and neuronal cultures: Characterization of binding sites and modulation of release by lymphokines and trophic factors. J Neurosci 12:1668–1678.

Avery RL, Pieramici DJ, Rabena MD, Castellarin AA, Nasir MA, Giust MJ. 2006. Intravitreal bevacizumab (Avastin) for neovascular age-related macular degeneration. Ophthalmology 113:363–372, e5.

Banin E, Dorrell MI, Aguilar E, Ritter MR, Aderman CM, Smith AC, Friedlander J, Friedlander M. 2006. T2-TrpRS inhibits preretinal neovascularization and enhances physiological vascular regrowth in OIR as assessed by a new method of quantification. Invest Ophthalmol Vis Sci 47:2125–2134.

Bernardos RL, Barthel LK, Meyers JR, Raymond PA. 2007. Late-stage neuronal progenitors in the retina are radial Muller glia that function as retinal stem cells. J Neurosci 27:7028–7040.

Caldwell RB, Bartoli M, Behzadian MA, El-Remessy AE, Al-Shabrawey M, Platt DH, Caldwell RW. 2003. Vascular endothelial growth factor and diabetic retinopathy: Pathophysiological mechanisms and treatment perspectives. Diabetes Metab Res Rev 19:442–455.

Chan-Ling T, Stone J. 1992. Degeneration of astrocytes in feline retinopathy of prematurity causes failure of the blood–retinal barrier. Invest Ophthalmol Vis Sci 33:2148–2159.

Das A, McGuire PG. 2003. Retinal and choroidal angiogenesis: Pathophysiology and strategies for inhibition. Prog Retin Eye Res 22:721–748.

Dorrell MI, Aguilar E, Friedlander M. 2002. Retinal vascular development is mediated by endothelial filopodia, a preexisting astrocytic template and specific R-cadherin adhesion. Invest Ophthalmol Vis Sci 43:3500–3510.

Dorrell MI, Aguilar E, Jacobson R, Yanes O, Gariano R, Heckenlively J, Banin E, Ramirez GA, Gasmi M, Bird A, Siuzdak G, Friedlander M. 2009. Antioxidant or neurotrophic factor treatment preserves function in a mouse model of neovascularization-associated oxidative stress. J Clin Invest 119:611–623.

Dorrell MI, Friedlander M. 2006. Mechanisms of endothelial cell guidance and vascular patterning in the developing mouse retina. Prog Retin Eye Res 25:277–295.

Dorrell MI, Otani A, Aguilar E, Moreno SK, Friedlander M. 2004. Adult bone marrow-derived stem cells utilize R-cadherin to target sites of neovascularization in the developing retina. Blood 103:3420–3427.

Eichler W, Yafai Y, Wiedemann P, Fengler D. 2006. Antineovascular agents in the treatment of eye diseases. Curr Pharm Des 12:2645–2660.

Ferrara N, Kerbel RS. 2005. Angiogenesis as a therapeutic target. Nature 438:967–974.

Friedlander M. 2005. Stem cells and retinal diseases. In: Ryan SJH, Hinton DR, Schachat AP, Wilkinson P, editors. Retina, 4th ed. Elsevier: London, p 23–32.

Friedlander M. 2007. Fibrosis and diseases of the eye. J Clin Invest 117:576–586.

Friedlander M, Dorrell MI, Ritter MR, Marchetti V, Moreno SK, El-Kalay M, Bird AC, Banin E, Aguilar E. 2007. Progenitor cells and retinal angiogenesis. Angiogenesis 10:89–101.

Fruttiger M, Calver AR, Kruger WH, Mudhar HS, Michalovich D, Takakura N, Nishikawa S, Richardson WD. 1996. PDGF mediates a neuron-astrocyte interaction in the developing retina. Neuron 17:1117–1131.

Gebicke-Haerter PJ, Bauer J, Schobert A, Northoff H. 1989. Lipopolysaccharide-free conditions in primary astrocyte cultures allow growth and isolation of microglial cells. J Neurosci 9:183–194.

Gerhardt H, Golding M, Fruttiger M, Ruhrberg C, Lundkvist A, Abramsson A, Jeltsch M, Mitchell C, Alitalo K, Shima D, et al. 2003. VEGF guides angiogenic sprouting utilizing endothelial tip cell filopodia. J Cell Biol 161:1163–1177.

Ishida S, Usui T, Yamashiro K, Kaji Y, Amano S, Ogura Y, Hida T, Oguchi Y, Ambati J, Miller JW, et al. 2003. VEGF164-mediated inflammation is required for pathological, but not physiological, ischemia-induced retinal neovascularization. J Exp Med 198:483–489.

Keller A, Nesvizhskii AI, Kolker E, Aebersold R. 2002. Empirical statistical model to estimate the accuracy of peptide identifications made by MS/MS and database search. Anal Chem 74:5383–5392.

Liu X, Mashour GA, Webster HF, Kurtz A. 1998. Basic FGF, FGF receptor 1 are expressed in microglia during experimental autoimmune encephalomyelitis: Temporally distinct expression of midkine and pleiotrophin. Glia 24:390–397.

Madan A, Penn JS. 2003. Animal models of oxygen-induced retinopathy. Front Biosci 8:d1030–d1043.

Maddox DE, Shibata S, Goldstein IJ. 1982. Stimulated macrophages express a new glycoprotein receptor reactive with Griffonia simplicifolia I-B4 isolectin. Proc Natl Acad Sci USA 79:166–170.

McLeod DS, D'Anna SA, Lutty GA. 1998. Clinical and histopathologic features of canine oxygen-induced proliferative retinopathy. Invest Ophthalmol Vis Sci 39:1918–1932.

McLeod DS, Taomoto M, Cao J, Zhu Z, Witte L, Lutty GA. 2002. Localization of VEGF receptor-2 (KDR/Flk-1) and effects of blocking it in oxygen-induced retinopathy. Invest Ophthalmol Vis Sci 43:474–482.

Ng EW, Shima DT, Calias P, Cunningham ET Jr, Guyer DR, Adamis AP. 2006. Pegaptanib, a targeted anti-VEGF aptamer for ocular vascular disease. Nat Rev Drug Discov 5:123–132.

Otani A, Dorrell MI, Kinder K, Moreno SK, Nusinowitz S, Banin E, Heckenlively J, Friedlander M. 2004. Rescue of retinal degeneration by intravitreally injected adult bone marrow-derived lineage-negative hematopoietic stem cells. J Clin Invest 114:765–774.

Otani A, Friedlander M. 2005. Retinal vascular regeneration. Semin Ophthalmol 20:43–50.

Otani A, Kinder K, Ewalt K, Otero FJ, Schimmel P, Friedlander M. 2002. Bone marrow-derived stem cells target retinal astrocytes and can promote or inhibit retinal angiogenesis. Nat Med 8:1004–1010.

Ozaki H, Seo MS, Ozaki K, Yamada H, Yamada E, Okamoto N, Hofmann F, Wood JM, Campochiaro PA. 2000. Blockade of vascular endothelial cell growth factor receptor signaling is sufficient to completely prevent retinal neovascularization. Am J Pathol 156:697–707.

Penn JS, Tolman BL, Lowery LA. 1993. Variable oxygen exposure causes preretinal neovascularization in the newborn rat. Invest Ophthalmol Vis Sci 34:576–585.

Provis JM, Leech J, Diaz CM, Penfold PL, Stone J, Keshet E. 1997. Development of the human retinal vasculature: Cellular relations and VEGF expression. Exp Eye Res 65:555–568.

Provis JM, Sandercoe T, Hendrickson AE. 2000. Astrocytes and blood vessels define the foveal rim during primate retinal development. Invest Ophthalmol Vis Sci 41:2827–2836.

Ritter MR, Banin E, Moreno SK, Aguilar E, Dorrell MI, Friedlander M. 2006. Myeloid progenitors differentiate into microglia and promote vascular repair in a model of ischemic retinopathy. J Clin Invest 116:3266–3276.

Robinson GS, Ju M, Shih SC, Xu X, McMahon G, Caldwell RB, Smith LE. 2001. Nonvascular role for VEGF: VEGFR-1, 2 activity is critical for neural retinal development. FASEB J 15:1215–1217.

Rohan RM, Fernandez A, Udagawa T, Yuan J, D'Amato RJ. 2000. Genetic heterogeneity of angiogenesis in mice. FASEB J 14: 871–876.

Rungger-Brandle E, Dosso AA, Leuenberger PM. 2000. Glial reactivity, an early feature of diabetic retinopathy. Invest Ophthalmol Vis Sci 41:1971–1980.

Smith LE. 2002. Pathogenesis of retinopathy of prematurity. Acta Paediatr 91(Suppl):26–28.

Smith LE, Shen W, Perruzzi C, Soker S, Kinose F, Xu X, Robinson G, Driver S, Bischoff J, Zhang B, et al. 1999. Regulation of vascular endothelial growth factor-dependent retinal neovascularization by insulin-like growth factor-1 receptor. Nat Med 5:1390–1395.

Smith LE, Wesolowski E, McLellan A, Kostyk SK, D'Amato R, Sullivan R, D'Amore PA. 1994. Oxygen-induced retinopathy in the mouse. Invest Ophthalmol Vis Sci 35:101–111.

Stalmans I, Ng YS, Rohan R, Fruttiger M, Bouche A, Yuce A, Fujisawa H, Hermans B, Shani M, Jansen S, et al. 2002. Arteriolar and venular patterning in retinas of mice selectively expressing VEGF isoforms. J Clin Invest 109:327–336.

Stone J, Itin A, Alon T, Pe'er J, Gnessin H, Chan-Ling T, Keshet E. 1995. Development of retinal vasculature is mediated by hypoxia-induced vascular endothelial growth factor (VEGF) expression by neuroglia. J Neurosci 15(7 Part 1):4738–4747.

Werdich XQ, McCollum GW, Rajaratnam VS, Penn JS. 2004. Variable oxygen and retinal VEGF levels: Correlation with incidence and severity of pathology in a rat model of oxygen-induced retinopathy. Exp Eye Res 79:623–630.

Witmer AN, Vrensen GF, Van Noorden CJ, Schlingemann RO. 2003. Vascular endothelial growth factors and angiogenesis in eye disease. Prog Retin Eye Res 22:1–29.

Yamada H, Yamada E, Ando A, Seo MS, Esumi N, Okamoto N, Vinores M, LaRochelle W, Zack DJ, Campochiaro PA. 2000. Platelet-derived growth factor-A-induced retinal gliosis protects against ischemic retinopathy. Am J Pathol 156:477–487.

Zachary I. 2005. Neuroprotective role of vascular endothelial growth factor: Signalling mechanisms, biological function, and therapeutic potential. Neurosignals 14:207–221.